DOI: 10.1002/ ((please add manuscript number))
Article type: Full Paper

Tunable White-Light Emission from Conjugated Polymer-Di-Ureasil Materials

*Niamh Willis-Fox, Mario Kraft, Jochen Arlt, Ullrich Scherf and Rachel C. Evans**

N. Willis-Fox, Dr. R. C. Evans
School of Chemistry and CRANN, Trinity College Dublin, The University of Dublin, Dublin 2, Ireland.
E-mail: raevans@tcd.ie
M. Kraft, Prof. U. Scherf
Makromolekulare Chemie, Bergische Universität Wuppertal, 42097 Wuppertal, Germany.
Dr. J. Arlt
Collaborative Optical Spectroscopy, Micromanipulation and Imaging 20 Centre (COSMIC) and SUPA, School of Physics, King's Buildings, University of Edinburgh, EH9 3JZ, U.K.

Keywords: Conjugated Polymers, Hybrid Materials, Optically Active Materials; Photoluminescence, Composites

Conjugated polymer (CP)-di-ureasil composite materials displaying a tunable emission color from blue to yellow, through white have been prepared using a simple sol-gel processing method. The tunability of the emission color arises from a combination of energy transfer between the di-ureasil and the CP dopant and the excitation wavelength dependence of the di-ureasil emission. Incorporation of the CP does not adversely affect the bulk or local structure of the di-ureasil, enabling retention of the structural and mechanical properties of the host. Furthermore, CP-di-ureasils display superior thermal and photostability compared to the parent CPs. Thermogravimetric analysis shows that the onset of thermal decomposition can be increased by up to 130 ˚C for CP-di-ureasils, while photostability studies reveal a significant decrease in the extent of photodegradation. Steady-state photoluminescence spectroscopy and picosecond time-resolved emission studies indicate that the observed tunable emission arises as a consequence of incomplete energy transfer between the di-ureasil and the CP dopant, resulting in emission from both species on direct excitation of the di-ureasil matrix. The facile synthetic approach and tunable emission demonstrate that CP-di-ureasils are a highly promising route to white-light-emitters that simultaneously improve the stability and reduce the complexity of CP-based multi-layer device architectures.

1. Introduction

Conjugated polymers (CPs) have demonstrated exceptional promise as an active component of flexible, light-weight organic electronic devices due to their favorable optoelectronic properties and solution processability.[1] The development of white-light emitting CP-based materials has attracted considerable interest due to their applications in next generation solid-state lighting,[2] back-lighting for liquid-crystal displays[3] and full-color flat-panel electroluminescence.[4] White-light emitting systems usually depend on the principle of additive color mixing, in which multiple components that emit either three primary colors (red, green and blue)[3, 5] or two complementary colors (*e.g.* blue and orange)[3] are combined. This requirement for multiple emissive species naturally gives rise to a multi-layer device architecture in which each layer emits a distinct color, which when combined produces white light.[6] The performance of CP-based electronic devices is inherently linked to the morphology of each CP layer.[7] As such, to prevent modification of the morphology of initially cast layers by those deposited subsequently, the use of orthogonal solvents is required.[8] Alternatively, initial layers must be rendered insoluble after deposition, by processes such as 'hard-baking' or cross-linking reactions.[9] This introduces a further level of complexity into the device fabrication process. To circumvent these challenges, polymer white-light emitting devices have been produced by blending either a range of different polymers or a single polymer host with a dopant molecular dye.[6] However, these systems suffer from intrinsic phase separation[2] and as such, there are increasing reports of white-emitting polymers in which several chromophores emitting in either the primary or complementary spectral regions are incorporated within a single polymer chain.[10] Recently, a step towards improved resolution in display devices has been achieved through the process of microcontact printing to design nanopixels composed of a blue-emitting polymer host coordinated to red (Eu(III)) and green (Tb(III)) emitting metal

complexes.[11] This technique of coordinating metal complexes to a polymer host has further been exploited to tune the emission color to produce white light by varying the conjugation length of the host polymer.[12] Nonetheless, these polymers present a significant synthetic challenge and do not overcome the inherent instability possessed by CP-based devices.

Encapsulation of CPs within an inorganic host material has been shown to enhance environmental stability[13] and provides an elegant route to indirectly manipulate the conformation and orientation of the polymer within the active layer.[14] However, the host material typically serves primarily to isolate or aggregate the polymer chains and makes limited contribution to the functional properties of the material. Recently, we have shown that upon incorporation of blue-emitting poly(fluorene) CPs within an organic-inorganic di-ureasil matrix there is clear evidence of synergistic interaction between the di-ureasil host and the CP dopant, resulting in a dramatic enhancement of the photoluminescence quantum yield.[15] Di-ureasils are comprised of a siliceous skeleton that is chemically-grafted to poly(ethylene oxide) (PEO)/poly(propylene oxide) (PPO) chains through two urea [NHC(=O)HN] cross-linkages (**Figure 1**).[16, 17] Di-ureasils are inherently photoluminescent and have been employed as an active host for lanthanide ions/complexes[18, 19] and molecular dyes,[20] in which the excitation wavelength dependence of the di-ureasil emission is exploited to modulate energy transfer between di-ureasil and dopant.[18, 21] Moreover, as organic-inorganic hybrids, di-ureasils should show improved chemical compatibility with CPs compared to a purely inorganic matrix, thereby reducing the risk of phase separation.

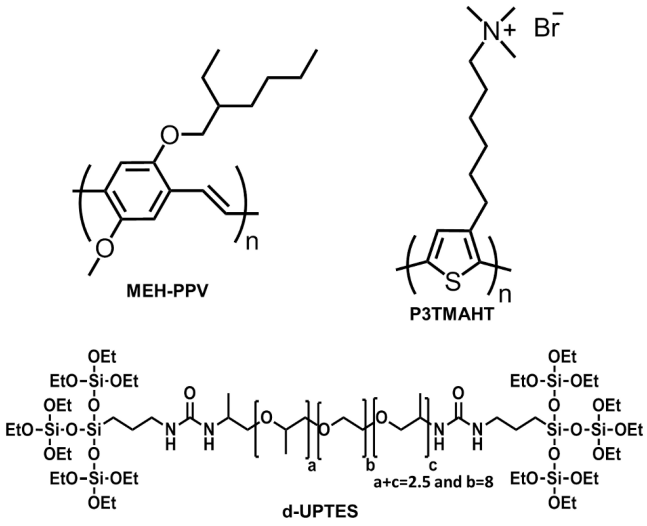

Figure 1. Chemical structures of the CPs investigated and the di-ureasil precursor, d-UPTES.

Here, we report the synthesis, structural characterization and optical performance of CP-di-ureasil materials incorporating the red-emitting poly(thiophene) P3TMAHT and the orange-emitting poly(phenylene) MEH-PPV (Figure 1) at different CP dopant concentrations. These CPs were selected based on the significant overlap of their absorption bands with the emission spectrum of the di-ureasil. We demonstrate that with judicious selection of the excitation wavelength and/or CP dopant concentration, the emission color of the CP-di-ureasil composite can be selectively tuned from the blue to the yellow spectral regions, passing through white, due to energy transfer. This is a significant advantage since it is synthetically complex to produce individual CPs exhibiting tunable emission.[22, 23] Moreover, incorporation of the CP within the di-ureasil host gives rise to improved thermal and photostability of the resulting active layer. Given the simple, solution-based fabrication method and the structural tunability of the two components, this approach presents a versatile and efficient route to highly desirable white-light emitting CP-di-ureasil materials, whose optoelectronic properties may be tuned across a wide spectral region.

2. Results and Discussion

2.1. Synthesis of CPE-di-ureasils

The synthesis of the di-ureasil host d-U(600) is well-described.[16, 17, 24] In brief, 3-isocyanatopropyltriethoxysilane, ICPTES, is reacted with Jeffamine ED-600 to form the intermediate di-ureapropyltriethoxysilane (d-UPTES) (Figure 1), which is subsequently subjected to acid-catalyzed hydrolysis and condensation of the siliceous groups to form the di-ureasil hybrid. In a typical synthesis, Jeffamine ED-600 (1 ml, 1.75 mmol) was dissolved in THF (5 ml), to which ICPTES (0.9 ml, 3.0 mmol) was added under stirring. This mixture was refluxed at 70 ˚C for 24 h to prepare the d-UPTES precursor solution. The undoped di-ureasil is obtained by addition of ethanol (0.409 ml, 7 mmol), HCl (0.5 M, 0.040 ml) and H_2O (0.095 ml, 5.3 mmol) to the d-UPTES solution, which triggers the acid-catalyzed sol-gel reaction. This corresponds to a ratio of 1 ICPTES: 2.3 EtOH: 1.8 H_2O: 0.006 HCl molar equivalents. CP-doped samples were prepared by the addition of a fixed volume of stock solution to the d-UPTES precursor prior to initiating the sol-gel reaction to obtain the requisite dopant concentration (wt%) described in **Table 1**. Following initiation of the sol-gel reaction, the solution was stirred for 5 min, before being poured into a polyurethane mold which was then covered with Parafilm. After 24 h, the Parafilm was pierced to encourage slow evaporation of the solvent for 24 h. The samples were then placed in the oven at 40 ˚C for 48 h to complete the drying process which produced free-standing, transparent monoliths. As the CP content increased, the monoliths became increasingly red in color.

Table 1. Composition of CP-di-ureasils prepared in this study. [CP] is the concentration of the CP stock solution (in mM repeat units (r.u.)) added to the d-UPTES. The incorporated CP weight percent (wt%) was estimated from [CP] and the mass of the dry CP-di-ureasil.

Polymer	Sample	[CP] [mM r.u.]	CP wt%
Undoped di-ureasil	d-U(600)	0.0	0

P3TMAHT	P3T-0.6	0.33	0.6×10^{-3}
	P3T-1.2	0.65	1.2×10^{-3}
	P3T-1.8	0.87	1.8×10^{-3}
	P3T-2.4	1.31	2.4×10^{-3}
	P3T-3.3	1.74	3.3×10^{-3}
	P3T-6.6	3.47	6.6×10^{-3}
MEH-PPV	MEH-0.2	0.15	0.2×10^{-3}
	MEH-0.5	0.30	0.5×10^{-3}
	MEH-0.7	0.40	0.7×10^{-3}
	MEH-1.0	0.45	1.0×10^{-3}
	MEH-1.3	0.81	1.3×10^{-3}
	MEH-2.7	1.62	2.7×10^{-3}

2.2. Bulk and local structure of CP-di-ureasils

The samples are designated as d-U(600) for the undoped di-ureasil, and MEH-x and P3T-x for MEH-PPV- and P3TMAHT-di-ureasils, respectively, where x represents the weight percent (10^{-3} wt%) of the CP incorporated (Table 1). **Figure 2** shows the PL spectrum of d-U(600) and the UV/Vis absorption spectra of MEH-PPV and P3TMAHT. Significant spectral overlap between the d-U(600) emission and the absorption bands of both CPs is observed, indicating that efficient resonance energy transfer from the di-ureasil donor (*D*) to the CP acceptor (*A*) may occur if they lie within the Förster radius.[25]

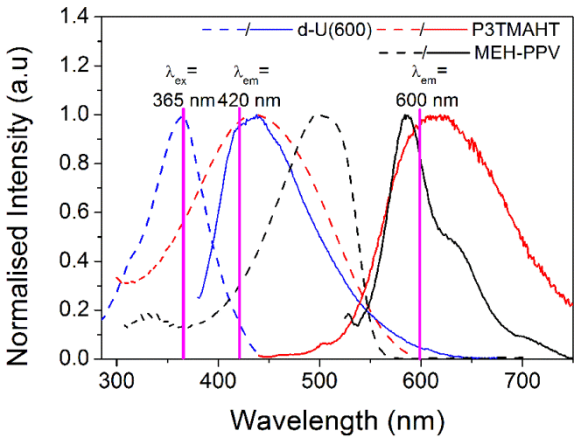

Figure 2. Emission and excitation spectra for d-U(600) (blue, λ_{ex} = 365 nm, λ_{em} = 420 nm) and UV/Vis absorption and emission spectra for MEH-PPV (black, λ_{ex} = 480 nm in THF) and P3TMAHT (red, λ_{ex}= 430 nm in aqueous solution). Emission spectra are shown as solid lines and excitation and UV/Vis absorption spectra are shown as dashed lines. The pink lines highlight the excitation (λ_{ex}) and emission (λ_{ex}) wavelengths used in the TCSPC experiments.

The distribution of the CP within the di-ureasil was first investigated using confocal microscopy. CP-di-ureasils were directly excited within the CP absorption band (λ_{ex} = 488 nm) and observed using a red filter which examines emission wavelengths in the range 550-740 nm (shown in **Figure S1a**, Supporting Information for P3T-6.6). Intense red emission was observed from isolated domains of *ca*. 2-5 μm diameter, which are homogeneously distributed within the di-ureasil matrix. Each domain is anticipated to comprise of multiple CP chains. Selective excitation of the di-ureasil (λ_{ex} = 405 nm) also resulted in the observation of red emission from the same isolated domains attributed to the CP. An overlay of the images collected on excitation of the di-ureasil and the CP, respectively, exhibits identical emission from the domains attributed to the CP, providing preliminary evidence for the occurrence of energy transfer from the di-ureasil host to the incorporated CP.

Structural characterization of the CP in the di-ureasil host is challenging due to the low dopant concentration. However, analysis of the di-ureasil itself may indirectly shed some light on the local environment of the CP within the host. The PXRD patterns for all samples exhibit a primary band centered at 21.1˚, with a shoulder at 11.0-15.0˚, which is typical of these highly amorphous materials (**Figure S2**, Supporting Information). The main peak at 21.1˚ is associated with the presence of ordering within the siliceous domains[21, 24, 26, 27], and from this, the structural unit distance, *d*, was determined to be 4.2 ± 0.1 Å (from Bragg's Law). The shoulder between 11.0˚ and 15.0˚ has previously been reported for similar di-ureasil samples prepared through carboxylic acid solvolysis and is attributed to in-plane ordering of other intra-siloxane

domains.[27] This gives rise to a characteristic distance of 3.4 ± 0.5 Å matching those reported previously. The coherent length over which the structural unit survives in the di-ureasil was estimated to be 11.1 ± 1 Å (from the Scherrer equation).[28] This value is similar to that previously reported for di-ureasils[24, 27] suggesting that the incorporation of the CPs, within the concentration range examined in this study, does not induce significant structural changes in the di-ureasil.

The ^{29}Si MAS-NMR spectra of all CP-di-ureasils studied contain three broad signals characteristic of T_1, T_2 and T_3 units (**Figure S3**, Supporting Information). These are labelled according to the conventional T_n notation, where n (n = 1, 2, 3) is the number of Si-bridging oxygen atoms, *i.e.* T_1 = (R′Si(OSi)-$(OR)_2$), T_2 = (R′Si$(OSi)_2$(OR)) and T_3 = (R′Si$(OSi)_3$). The T_2 and T_3 signals (at –58.1 ppm and –66.6 ppm, respectively) are the dominant environments with a negligible contribution from T_1 at –49.4 ppm, as is the case for lanthanide complex doped di-ureasils.[21] The absence of the T_0 signal confirms that there is no unreacted precursor remaining.[21] The degree of condensation, *C*, of the siliceous network was determined from *C* (%) = 1/3(%T_1 + 2%T_2 + 3%T_3), using Gaussian deconvolution of the peaks to determine the relative population of each organosiloxane species (see **Table S1**, Supporting Information). The *C* values obtained [73-83%] are in good agreement with those previously observed for poly(fluorene)-di-ureasils.[15] No linear relationship between *C* and wt% of CP incorporated is observed, even with the much higher molecular weight MEH-PPV. This is contrary to previous studies with lanthanide complexes of varying sizes in which the degree of condensation decreased with increasing complex size.[29] This is most likely due to the differing level of interaction between the CP and the di-ureasil. In particular the di-ureasil is able to interact strongly with Eu^{III}-containing complexes *via* the incorporation of its C=O groups into the coordination sphere of the metal complex,[29] a situation that is impossible for the non-metal containing CPs

investigated here. The ^{13}C CP/MAS-NMR spectra are in excellent agreement with those previously reported for di-ureasils of this type[27] (**Figure S4**, Supporting Information) further indicating that the hybrid structure is not chemically modified upon CP incorporation.

The FTIR spectra of the CP-di-ureasils (**Figure S5**, Supporting Information) match those of undoped di-ureasils.[21, 26] The Amide I band of the FTIR spectra represents the specificity and degree of hydrogen bonding interactions associated with C=O stretching frequencies in different local environments.[17] Gaussian deconvolution of the Amide I region (1610-1770 cm^{-1}) of the spectra yielded three components at 1714, 1667 and 1638 cm^{-1} (**Figure S6**, Supporting Information for P3T-1.8). The first two of these bands are ascribed to the vibrations of C=O groups within disordered hydrogen-bonded urea-polyether associations of increasing strength, while the component at 1638 cm^{-1} is attributed to strong self-associated hydrogen-bonded urea-urea associations.[17, 21, 26] There is no noticeable change in the position or contribution of any of these bands as a function of CP concentration, suggesting no significant effect on hydrogen bonding interactions within the di-ureasil on CP incorporation (see **Table S3**, Supporting Information).

2.3. Improved stability of the CP within the di-ureasil matrix

The thermograms for d-U(600) match those previously reported,[19, 30, 31] with the onset of sample decomposition at ~339 ˚C (**Figure 3a**). The thermograms of both CPs exhibit two major decomposition events, at 220 and 435 ˚C for P3TMAHT and 300 and 508 ˚C for MEH-PPV, in good agreement with previous reports for MEH-PPV[32] and the related poly(3-hexylthiophene) P3HT.[33] The first step is attributed to the loss of side chains attached to the polymer backbone, while the second is associated with decomposition of the conjugated polymer backbone. Doping of related ED-900-based di-ureasils with lithium salts has previously been shown to thermally destabilize the matrix.[30] However, for P3T-di-ureasils, incorporation of the CP yields a material that has a significantly higher thermal stability than

the CP alone with the main decomposition occurring at ~335 ˚C (Figure 3a), which represents an increase in thermal stability of ~120 ˚C. Since MEH-PPV has an intrinsically higher thermal stability than P3TMAHT, this effect is less pronounced for MEH-di-ureasils, with the onset of thermal decomposition increasing by ~30 °C (**Figure S7**, Supporting Information). No direct relationship between the CP doping wt% and the improvement in the thermal stability is observed (**Table S4**, Supporting Information).

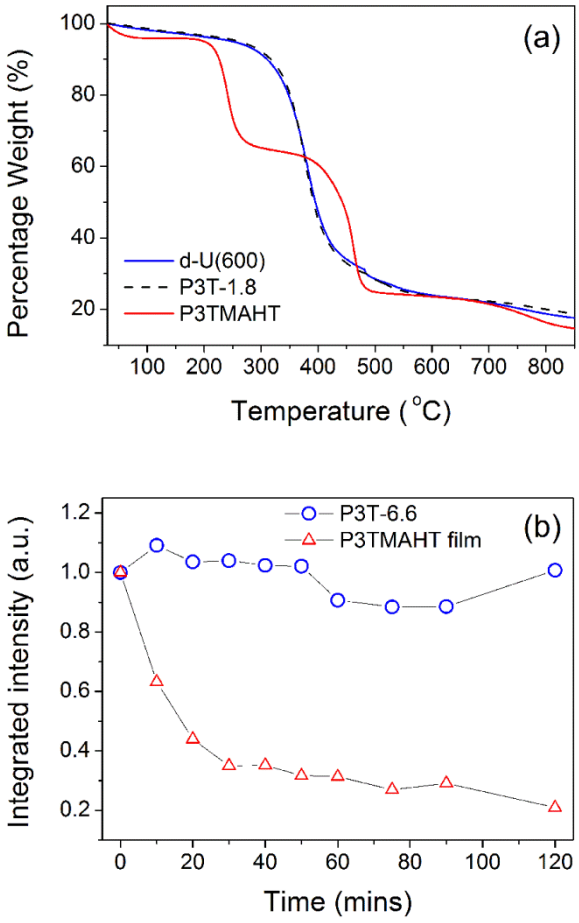

Figure 3. (a) TGA thermograms of d-U(600) (blue solid line), P3T-1.8 (black dashed line) and pure P3TMAHT (red solid line). TGA measurements were performed in air at a heating rate of 10 ˚C/min. (b) Integrated emission intensity of a pure P3TMAHT thin film on glass (open red triangles) and P3T-6.6 (open blue circles) under irradiation at 450 nm. The black lines serve only to guide the eye.

The photostability of the CP-di-ureasils was also investigated. Figure 3b shows the integrated emission intensity of P3T-6.6 and a pure P3TMAHT film as a function of irradiation time upon excitation at 450 nm. The integrated intensity of the P3TMAHT film dropped rapidly during the first 30 min of irradiation to 30% of the initial value, and continued to decrease steadily to 20% at the end of the irradiation period (2 h). This is in stark contrast to the integrated emission intensity of the P3T-6.6 sample, which remains almost constant throughout the observation window. Similar trends were observed on comparison of MEH-2.7 and the MEH-PPV film (**Figure S8**, Supporting Information); however it should be noted that the MEH-PPV film was less susceptible to photodegradation, dropping to 55% of the initial value within the 2 h period. Polythiophenes and PPV-type polymers are both susceptible to chemical attack under UV/visible irradiation; however the archetypical polythiophene P3HT is typically more stable than MEH-PPV.[34] The origin of the reduced photostability of the P3TMAHT film is unclear at present, but it is possible that the ionic side groups of the polyelectrolyte may promote photodegradation, for example by expediting the diffusion of oxygen and/or water into the film. However, the photostability of both MEH-PPV and P3HT can be improved on blending with other species, such as fullerenes,[35a] graphene oxide[35b] or other polymers[35c] which facilitate the trapping of reactive intermediates. The enhanced photostability observed here for MEH- and P3T-di-ureasils is most likely to result from a similar mechanism.

2.4. Steady-state photoluminescence properties – energy transfer and the generation of white-light emission

The PL spectra of d-U(600) as a function of excitation wavelength are shown in **Figure 4a**. The emission maximum is strongly dependent on the excitation energy, red-shifting to longer wavelengths as λ_{ex} increases. A similar trend is observed in the corresponding excitation spectrum (**Figure S9a**, Supporting Information). This behavior is typical of di-ureasils and has previously been attributed to the convolution of donor-acceptor

pair recombinations occurring in the NH/C=O groups of the urea linkages and in the oxygen-related defects in the siliceous nanodomains.[24, 36] The component at 2.9–2.2 eV (blue band) is ascribed to photoinduced proton transfer between the urea linkages, while a second component at 3.3–2.8 eV (purple-blue band) is assigned to defects within the siliceous nanodomains.[24, 36]

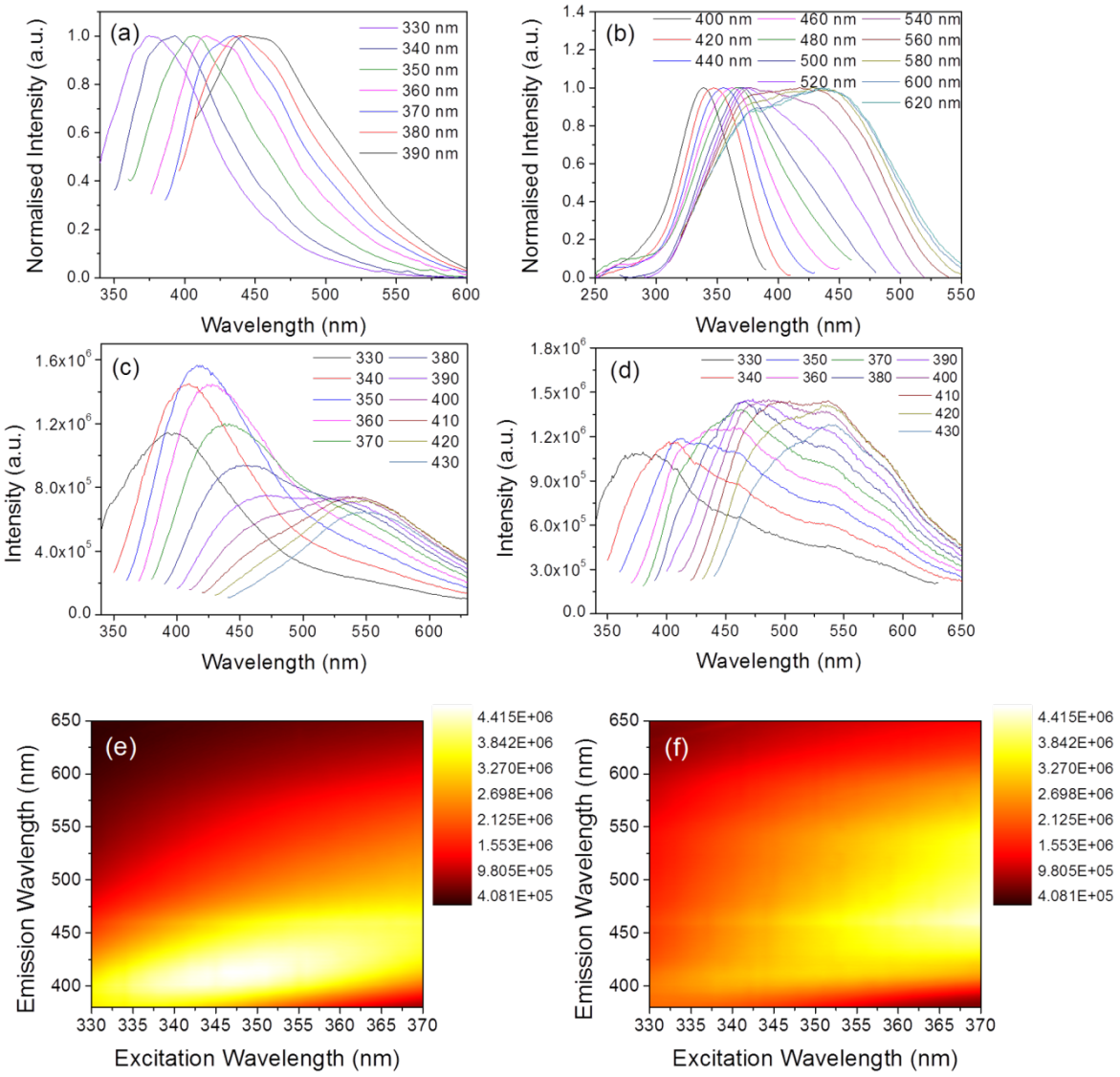

Figure 4. (a) PL spectra (λ_{ex} = 330, 340, 350, 360, 370, 380 and 390 nm) of d-U(600). (b) PL excitation spectra (λ_{em} = 400, 420, 440, 460, 480, 500, 520, 540, 560, 580, 600 and 620 nm) of P3T-1.8. (c) PL spectra (λ_{ex} = 330, 340, 350, 360, 370, 380, 390, 400, 410, 420 and 430 nm) of P3T-1.8. (d) PL spectra (λ_{ex} = 330, 340, 350, 360, 370, 380, 390, 400, 410, 420 and 430 nm) of MEH-0.5. Emission-excitation matrices for (e) P3T-1.8 and (f) MEH-0.5, where λ_{ex}= 330–370 nm and λ_{em}= 380–650 nm (both at 1 nm intervals). All measurements were performed at room temperature.

Di-ureasils have been shown to act as efficient energy donors while acting as host matrices for diverse lanthanide ions, complexes and nanoparticles.[18, 19, 37] In conjugated polymers, excitation energy transfer between donors (*D*) and acceptors (*A)* is favored by Förster-type resonance energy transfer (FRET) based on long-range dipole-dipole interactions,[25, 38] which requires a strong overlap between donor emission and the acceptor absorption spectra.[25] As described earlier, this condition is met by the di-ureasil donor and CP acceptor pairs chosen here (Figure 2). The FRET efficiency is also highly dependent on the center to center distance between *D* and *A*.[38] The spectral overlap integral, J_{DA}, was quantified for both di-ureasil-CP pairs from:

$$J_{DA}(\lambda) = \int_0^\infty F_D(\lambda)\varepsilon_A(\lambda)\lambda^4 d\lambda \quad (1)$$

where F_D is the intensity of the donor emission spectrum at wavelength λ to $\lambda+\Delta\lambda$, with the total intensity normalized to unity and ε_A is the molar absorption coefficient at wavelength λ. Using J_{DA}, the Förster distance, R_0, the distance at which the FRET efficiency is 50% efficient, can be calculated from:

$$R_0^6 = \frac{9000(ln10)\kappa^2\Phi_D J_{DA}}{128\pi^5 n^4 N_A} \quad (2)$$

where Φ_D is the photoluminescence quantum yield of the donor, n is the refractive index of the host di-ureasil (1.5)[39] and κ is the orientation factor describing the relative orientation of the transition dipoles of the donor and acceptor. Due to the amorphous nature of the material, κ was taken to be 2/3, which is appropriate for dynamic random averaging of the donor and acceptor.[25] The calculated spectral overlap integrals and Förster distances are shown in **Table 2**. The Förster distances are slightly smaller than those found for systems of blended polymers in which MEH-PPV acts as the acceptor, which range from R_0 ~5.1 nm when poly(*N*-vinylcarbazole) acts as the energy donor[38] to ~6 nm when poly(9,9-di-*n*-octylfluorenyl-2,7-dil) is the donor.[40] However, the R_0 values obtained here are very similar

to those obtained for energy transfer from oligonucleotides to a zwitterionic polythiophene derivative (R_0 = 2.54 – 2.68 nm).[41]

Table 2. Calculated spectral overlap integrals, $J_{DA,}$ and Förster radii, $R_{0,}$ for P3TMAHT and MEH-PPV with the d-U(600) host.

CP	J_{DA} [M^{-1} cm^3]	R_0 [nm]
P3TMAHT	1.5×10^{-14}	2.3
MEH-PPV	2.7×10^{-14}	3.7

Figure 4c and 4d show the PL spectra for P3T-1.8 and MEH-0.5 as a function of excitation wavelength, as representative samples for each system (see Figure 4b and S9b for corresponding excitation spectra). On addition of the CPs to the di-ureasil host matrix, the PL spectra retain a broad emission band in the blue spectral region, whose excitation wavelength dependence indicates that it may be ascribed to the di-ureasil emission. Previously, energy transfer from a di-ureasil host to a dopant species has been inferred from the presence or absence of the di-ureasil band in the emission spectrum.[18, 42] For di-ureasils doped with an Eu(1-(2-napththyl)-4,4,4-trifluoro-1,3-butanedionate)$_3$·2,2'-bipyridine complex the di-ureasil emission is completely absent,[42] while this phenomenon occurs only at high dopant concentrations for the analogous Cu(CF_3SO_3)$_3$-di-ureasils, suggesting that energy transfer is less efficient in the latter system.[18] The detection of the di-ureasil emission in the PL spectra of MEH- and P3T-di-ureasils suggests incomplete energy transfer in this case. This is advantageous as the di-ureasil emission provides a significant contribution to the total sample emission, which is necessary for the generation of white light. The emission spectra also exhibit a broad emission band in the orange-red spectral region, which is attributed to emission from the CP. The emission maximum of this band is relatively insensitive to the excitation wavelength.

It should be noted that at low dopant concentrations the CP emission maximum is significantly blue-shifted upon incorporation into the di-ureasil compared to the parent stock solutions (~65 and 75 nm for P3TMAHT and MEH-PPV, respectively). However, as the CP dopant wt% is increased, the emission maximum subsequently red-shifts (**Figure S10**, Supporting information). Conjugated polymers and polyelectrolytes are well-known to form molecular clusters or aggregates in poor solvents due to solvophobic interactions between individual polymer chains.[43] These aggregates can be broken-up through the addition of a more favorable co-solvent[23, 44] or surfactants,[43, 45] which can be experimentally observed by a blue-shift in the emission maximum due to the decreased effective conjugation length.[44] Similarly large spectral shifts have been reported for the P3TMAHT emission band in a related di-block copolymer upon interaction with DNA, which changes the aggregate structure.[46] A large blue-shift (86 nm) in the emission maximum has also previously been observed on incorporation of MEH-PPV into a PVK matrix.[47] As expected the magnitude of the emission signal in the red region of the spectrum increases with increasing CP dopant concentration (**Figure S11** and **S12** for P3T-di-ureasils and **Figure S13** and **S14** MEH-di-ureasils, Supporting Information).

It is important to note that the spectral overlap for di-ureasil-MEH-PPV is almost twice that calculated for the di-ureasil-P3TMAHT combination (Table 2), suggesting the energy transfer to MEH-PPV should be more efficient. However, in the case of both CPs studied here, we note that the absorption band of the CP partially overlaps with that of the di-ureasil (310-450 nm). As such, at these wavelengths, selective excitation of the di-ureasil is not possible. However, at the lowest excitation wavelengths (250-380 nm), where the CP absorption is minimal, significant CP emission is still observed, further suggesting the existence of energy transfer.

The excitation spectra for P3T- and MEH-di-ureasils monitored specifically in the CP emission region (500–580 nm) exhibit a major component centered at 430-450 nm assigned to direct CP excitation (Figure 4b and Figure S9b). However, a shoulder at ~370 nm is also observed, which is reminiscent of the d-U(600) excitation band (Figure S9a). The contribution from this shoulder increases as the monitoring wavelength is moved towards the di-ureasil emission range (400-440 nm), further supporting this assignment. The presence of this di-ureasil band in the excitation spectrum while monitoring the CP emission, even at the highest CP concentrations examined (see Figure S12d and S14d), supports the occurrence of di-ureasil to CP energy transfer.[18]

Figure 4e and 4f show the emission-excitation matrices (EEMs) for P3T-1.8 and MEH-0.5, respectively. EEMs plot the emission spectrum of the sample as a function of excitation wavelength as a 2D color map, where different colors represent variations in the emission intensity and not the emission color. The EEMs illustrate that through careful selection of the excitation wavelength, the resulting emission of the CP-di-ureasil can be tuned across the entire visible spectrum. The EEM of P3T-1.8 (Figure 4e) shows emission from the di-ureasil host in the region 380 to 475 nm (λ_{ex}= 330-370 nm), which reaches a maximum at λ_{ex}= 350 nm and then subsequently reduces in intensity. Moreover, there is an increase in the emission originating from the CP in the green-red region (475-625 nm) as the excitation wavelength increases. The reduction in di-ureasil emission at λ_{ex}>350 nm, accompanied by the increase in CP emission leads to similar emission intensity across the emission range investigated. The EEM of MEH-0.5 (Figure 4f) is slightly different as the CP emission dominates the entire emission spectrum, which increases in intensity across the excitation wavelength range studied (330-370 nm). However, the di-ureasil contribution is still visible for MEH-0.5 between 420-480 nm. This band merges with the CP emission at λ_{ex}>350 nm, again leading to similar emission intensity across the emission range investigated at higher excitation wavelengths.

Figure 5 plots the Commission Internationale d'Éclairage (CIE) 1931 *xy* chromaticity diagrams for representative P3T- and MEH-di-ureasils as a function of excitation wavelength and CP doping wt%. The CIE chromaticity diagram is a color space designed to represent all the colors perceived by a human eye.[48, 49] Color-matching functions, which are related to the response of the cones in a human eye, are used to represent the profile of a given emission spectrum as a set of (*x, y*) color coordinates on the CIE chromaticity diagram.[48] Taking P3T-1.8 as an example, Figure 5a shows that by taking advantage of the excitation wavelength dependence of the di-ureasil emission, the emission color can be tuned from the blue (0.19, 0.16) to the yellow (0.31, 0.43) region, through white (0.23, 0.30). As the excitation wavelength is increased, the 'blue' emission of the di-ureasil is shifted towards the red spectral region where the CP emits; when the contributions from both CP and di-ureasil are roughly equal, white-light is produced. Moreover, if the excitation wavelength is fixed (370 nm), and the CP dopant wt% is varied, the emission of the CP-di-ureasil can be modulated further (see Figure 5b for the P3T-x series). At low dopant concentrations, the di-ureasil emission dominates, giving rise to CIE *x,y* coordinates in the blue region (0.21, 0.20). As the CP concentration is increased, emission in the red gamut becomes more important, shifting the color coordinates to (0.39, 0.44), through white (0.29, 0.31). Figure 5c shows comparable trends with excitation wavelength and dopant concentration for the MEH-x series. As the MEH-PPV concentration increases the color coordinates move from blue to yellow on a path that passes increasingly close to pure white light, (0.33, 0.33).[49] However, this effect appears to saturate at a dopant concentration of 0.007 wt%.

Combined emission from direct excitation of the di-ureasil host and the CP emission resulting from *D-A* energy transfer gives rise to a broad emission band covering the majority of the visible spectrum. Judicious selection of the excitation

wavelength and CP dopant concentration provide two independent modes for tuning the emission color of CP-di-ureasils to generate a white-light emitting material. The photographs in Figure 5d and 5e show the white-light produced from P3T-1.8 (cool) and MEH-2.7 (warm), respectively, upon excitation at 385 nm. This approach provides a simple and elegant method to produce a single layer, white-light emitting material.

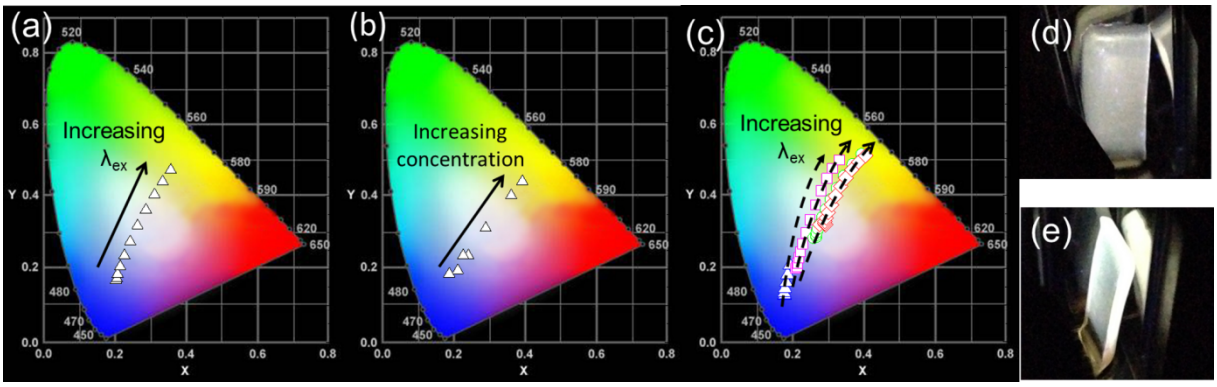

Figure 5. CIE *x,y* chromaticity diagrams for (a) P3T-1.8 as a function of increasing excitation wavelength (λ_{ex} = 330, 340, 350, 360, 370, 380, 390, 400, 410, 420 and 430 nm); (b) d-U(600), P3T-0.6, P3T-1.2, P3T-1.8, P3T-2.4, P3T-3.3 and P3T-6.6 at a fixed excitation wavelength (λ_{ex} = 370 nm); (c) MEH-0.0 (open triangles), MEH-0.2 (open squares), MEH-0.7 (open circles) and MEH-2.7 (open diamonds) as a function of excitation wavelength (MEH-0.0: λ_{ex} = 330, 340, 350, 360, 370, 380, 390 nm; MEH-0.2, MEH-0.7 and MEH-2.7: λ_{ex} = 330, 340, 350, 360, 370, 380, 390, 400, 410, 420 and 430 nm). The dashed arrows serve only to guide the eye. Photographs of (d) P3T-1.8 and (e) MEH-2.7 under UV-illumination (λ_{ex} = 385 nm).

2.4. Picosecond time-resolved emission studies

As indicated above, both CPs also absorb light to some extent at the wavelengths used to directly excite the di-ureasil. Thus, to further investigate the origin of the CP emission, (host-guest energy transfer *vs.* direct excitation), picosecond-time correlated single photon counting (ps-TCSPC) experiments were carried out. Fluorescence decays were measured for the P3T-x and MEH-x series, upon excitation at 365 nm and detection at 420 and 600 nm, which correspond predominantly to the di-ureasil and CP emission, respectively (Figure 2). All decay curves displayed complex multi-exponential behavior, requiring a minimum of three exponential components to

fit the data. In some instances it was not possible to obtain satisfactory fits to the data at short times after the pulse (<90 ps). This arises due to the nature of the samples themselves, which makes it impossible to completely eliminate contributions from scattering at the shortest timescales. For these samples, tail fits to the decay curves were used instead. Further information on the fitting procedure and all decay curves and fitting data can be found in the ESI.

Figure 6 presents the decay curves and fits obtained for d-U(600), P3T-6.6 and MEH-2.7 at room-temperature. d-U(600) exhibits a tri-exponential decay curve at λ_{em} = 420 nm, with components at τ_{dU1} ~ 400 ps, τ_{dU2} ~ 2.5 ns and τ_{dU3} ~ 9.9 ns. These lifetimes are extremely similar to those reported for undoped di-ureasils prepared *via* formic acid[26] and hydrochloric acid solvolysis.[15] The pre-exponential factors (α_i) show that τ_{dU1} is the primary component in the emission decay (α_{dU1} ~0.75), with τ_{dU2} (α_{dU2} ~0.20) and τ_{dU3} (α_{dU3} ~0.05) providing lesser contributions. Fluorescence decays for the CPs in solution were measured upon excitation at 460 nm and monitoring at 600 nm, the spectral region dominated by the CP emission (**Figure S16**, Supporting Information). The decays also exhibit complex tri-exponential behavior, comprised of a long lifetime component (τ_{CP3}) of ~600 ps for P3TMAHT and ~800 ps for MEH-PPV, ascribed to emission from isolated polymer chains,[50, 51] an intermediate lifetime (τ_{CP2}) of ~200 ps attributed to radiative relaxation of aggregated polymer species[50, 51], and a short component (τ_{CP1}) of ~25 ps. Very short lifetimes (~10-30 ps) have previously been assigned to conformational relaxation and/or energy migration along the polymer chain.[50, 52]

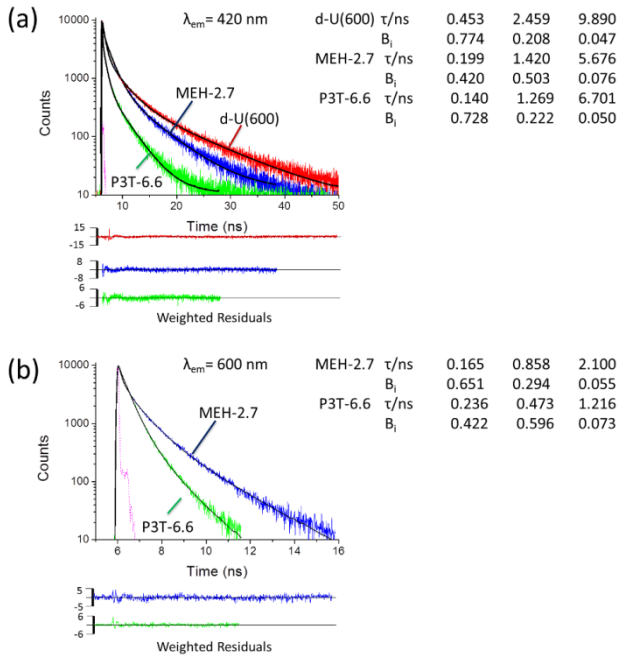

Figure 6. PL emission decay curves for (a) d-U(600) (red), MEH-2.7 (blue) and P3T-6.6 (green) detected at λ_{em} = 420 nm and (b) MEH-2.7 (blue) and P3T-6.6 (green) detected at λ_{em} = 600 nm. The resulting decay times (τ), fits (black lines), weighted residuals and instrument response function (IRF, pink dash) are also shown. λ_{ex} = 365 nm. All measurements were performed at room temperature.

Addition of P3TMAHT or MEH-PPV to the di-ureasil host results in a significant decrease in the lifetime measured at λ_{em}= 420 nm (Figure 6a). **Figure 7** shows the lifetimes and pre-exponential contributions obtained for multi-exponential fits to the P3T-x series. Over the concentration range examined, τ_{dU3} decreases considerably from 9.9 ns in the pure di-ureasil to 6.7 ns at the highest CP wt% for the P3T-x series (Figure 7a). The two shorter di-ureasil species remain reasonably constant with the exception of the highest P3TMAHT concentration (6.6×10^{-3} wt%), where τ_{dU1} drops considerably to 140 ps.

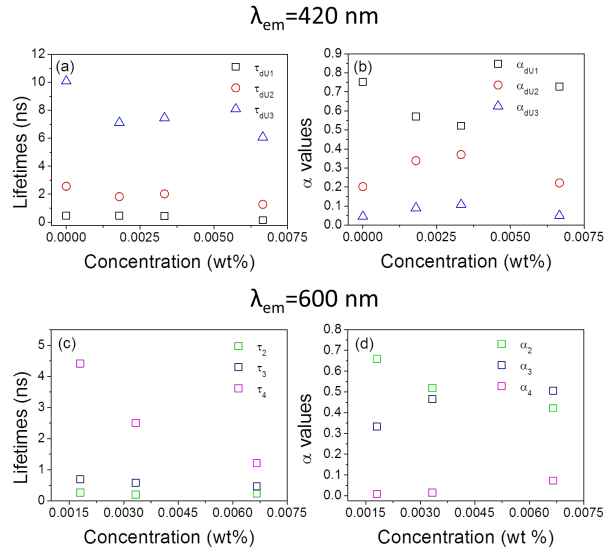

Figure 7. Emission lifetimes (τ_i) and corresponding pre-exponential factors (α_i) determined from tri-exponential fits to the fluorescence decays measured for the P3T-x series at (a, b) λ_{ex} = 365 nm and λ_{em} = 420 nm (di-ureasil emission) and (c, d) λ_{ex} = 365 nm and λ_{em} = 600 nm (CP emission band).

Similar trends are observed for MEH-x for both τ_i and α_i upon detection at 420 nm (see **Table S7**). The apparent decrease in the emission lifetime of the di-ureasil donor in the presence of the CP acceptor is clear evidence for the occurrence of energy transfer. The strong dependence of τ_{dU3} on CP concentration upon detection in the di-ureasil emission band further supports energy transfer between the two species.

The decay curves measured at 600 nm for the P3T-x series also require tri-exponential fits, whose lifetimes are denoted as τ_2, τ_3, and τ_4. The shortest lifetime component observed for the CP in solution, τ_{CP1}, disappears and is replaced by a fourth long-lived species, τ_4, which provides a minor contribution to the overall decay (~1%) (Figure 6b and Figure 7d). This long lifetime component (4.4 ns) is significantly longer than typically observed for CPs and is more reminiscent of the longest-lived di-ureasil component (τ_{dU3}). Although the CP emission dominates at this monitoring wavelength, there may be some residual emission from the di-ureasil present, making it reasonable to assign τ_4 to this contribution. Similar lifetimes have previous been observed by us for poly(fluorene)-doped di-ureasils.[15] The magnitude of

τ_4 decreases significantly from 4.4 ns to 1.2 ns as the CP wt% increases (Figure 7c), suggesting increasingly efficient energy transfer from the di-ureasil to the CP. The fact that the di-ureasil continues to contribute to the emission at 600 nm makes it difficult to unequivocally assign the lifetime components to individual emitting species. However, when comparing the lifetimes of the parent CP stock solutions and the corresponding CP-di-ureasils, it is noted that both the shortest component, τ_2 (which resembles and may contain a contribution from τ_{CP2}) and the intermediate lifetime, τ_3 (which is similar to τ_{CP3}), decrease steadily with increasing CP concentration. The decreases in τ_2 and τ_3 with increasing concentration thus suggest an increase in CP aggregation. This is supported by the PL spectra which suggest an initial deaggregation of the polymer species upon incorporation into the di-ureasil at the lowest concentration, followed by re-aggregation with increasing CP concentration (Figure S10, Supporting Information). This is similar to the behavior previously reported for MEH-PPV in a PVK matrix.[47] Similar trends in τ_i and α_i are observed for the MEH-x series upon detection at 600 nm (**Table S8**). However, τ_4 is much shorter for MEH-PPV (3.1 ns), suggesting more efficient energy transfer in this system, which is in line with the larger spectral overlap integral.

The occurrence of energy transfer within a system is often indicated by a rise time detected in the decay profile of the acceptor species. Energy transfer from highly planarized, aggregated chain segments of MEH-PPV to disordered, unaggregated chain segments has been shown to occur on a <1 ps timescale.[53] Thus, the lack of a rise time in decay curves measured here does not indicate an absence of energy transfer, but rather that it occurs on a timescale that is beyond the resolution of our experimental set-up. Overall, the ps-TCSPC data suggest that the origin of the CP emission is not solely due to direct excitation, but also arises due to host-guest energy transfer.

3. Conclusion

In summary, we have demonstrated a straightforward strategy for the preparation of CP-di-ureasils exhibiting a tunable emission color using a simple one-pot solution process. Our approach offers several synthetic advantages including green processing conditions (room-temperature, aqueous/alcohol solvents, low cost reagents) and no purification. Bulk structural characterization by PXRD and MAS-NMR revealed that incorporation of the CPs does not adversely affect the bulk or local structure of the di-ureasil, allowing the bulk samples to retain the structural and mechanical properties of the organic-inorganic hybrid host. Moreover, P3T- and MEH-di-ureasils exhibit significantly superior thermal and photostability in comparison to the parent conjugated polymers, providing a route to light-emitting materials with an enhanced shelf-life. Although large spectral overlap integrals were calculated for the d-U(600) host with both MEH-PPV and P3TMAHT, incomplete energy transfer from the di-ureasil host to the CP dopant results in emission from both species on direct excitation of the di-ureasil matrix. Judicious selection of the excitation wavelength or concentration of the CP dopant can be used to modulate the relative contribution of each component. The corresponding CIE chromaticity diagrams revealed that this approach can be used to tune the emission color from the blue to the yellow spectral regions, along a trajectory that passes through white. While we have focused on MEH-PPV and P3TMAHT here, the versatility of our synthetic approach means that it should be possible to introduce representatives from the variety of families of conjugated polymers available both commercially and through custom synthesis, providing a straightforward route to CP-di-ureasil composites exhibiting highly tunable optical properties. Moreover, in addition to the monolithic samples reported here, it is also possible to spin-coat the CPE-d-UPTES precursor solution as a homogeneous thin film onto different substrates. We are currently exploring this approach for the preparation of light-emitting and other optical devices. The facile synthetic approach, improved thermal and photostability of the resulting composite, the possibility to cast from solution as a single layer

film and the tunable emission color demonstrate that CP-di-ureasils are a versatile and efficient route to highly desirable white-light-emitters.

4. Experimental Section

Materials: Poly(propylene glycol)-block-poly(ethylene glycol)-block-poly(propylene glycol)-*bis*-(2-aminopropylether) (Jeffamine ED-600), 3-isocyanatoproplytriethoxysilane (ICPTES), ethanol (HPLC grade), hydrochloric acid (37% puriss), potassium bromide (FTIR grade), tetrahydrofuran (THF) (HPLC grade), toluene (reagent grade) and methanol (analytical grade) were purchased from Sigma Aldrich and used as received. Poly[2-methoxy-5-(2-ethylhexyloxy-1,4-phenylenevinylene) (MEH-PPV, M_n >100,000) was purchased from American Dye Source, Inc. and used as received. Poly[3-(6-triethylammoniumhexyl)thiophene]bromide (P3TMAHT) was synthesized as previously reported[45, 54] with an M_n of 12,000 g mol^{-1} by gel permeation chromatography (GPC) measured for the polymer precursor with bromohexyl side chains. We note that direct molecular weight measurement of the cationic P3TMAHT is not possible due to strong interaction of the CPE with the GPC column.

Instrumentation: Fourier Transform Infrared (FTIR) spectra were recorded on a Perkin-Elmer spectrum 100 FTIR spectrometer at room temperature. All FTIR spectra were collected over 4000-400 cm^{-1} by averaging 64 scans at a resolution of 4 cm^{-1}. The samples (2 mg) were finely ground and mixed with potassium bromide (175 mg) and pressed into pellets. To evaluate the contributions to the Amide I envelope spectral deconvolution was carried out using the Origin package and Gaussian band shapes in the region 1610-1770 cm^{-1}. Powder X-ray diffraction (PXRD) patterns were recorded using a Siemens D500 diffractometer. Samples were exposed to Cu K_α radiation (λ =1.54 Å) at room temperature in the range 5-70° (2θ).

Solid-state ^{29}Si and ^{13}C cross polarized (CP) and directly polarized (DP) nuclear magnetic resonance (NMR) spectroscopy were undertaken by the Engineering and

Physical Sciences Research Council (EPSRC) National Solid-State NMR service at the University of Durham, at ambient temperature on a Varian VNMRS instrument operating at 79.435 MHz for ^{29}Si and 100.56 MHz for ^{13}C. Spectra were recorded against an external tetramethylsilane (TMS) standard with magic angle spinning (MAS) at a spinning rate of 4300-5000 Hz. ^{13}C CP spectra were obtained as single contact experiments with a contact time of 5 ms and a recycle delay of 1.0 s (700 repetitions).

Thermogravimetric analysis (TGA) was performed using a Perkin Elmer Pyris 1 TGA thermogravimetric analyzer in the range 30-900 °C in an air atmosphere using *ca*. 2-5 mg sample, at a heating rate of 10 °C min^{-1} in a ceramic crucible. The instrument was calibrated against In and Ni standards in an air atmosphere.

Steady-state photoluminescence (PL) spectroscopy was performed on a Fluorolog-3 spectrophotometer (Horiba Jobin Yvon), using the front-face configuration for solid-state samples and an R9281x photomultiplier tube as the detector. Emission and excitation spectra were corrected for the wavelength response of the system and the intensity of the lamp profile over the excitation range, respectively, using correction factors supplied by the manufacturer. Emission and excitation slit widths were fixed at 2.5 nm. The sample XYZ tristimulus values and *xy* color coordinates were calculated from corrected emission spectra at 5 nm intervals as described previously.[48, 55]

Photostability studies were carried out on selected CP-di-ureasils and thin films of the pure CP samples. CP thin films were prepared by spin-coating P3TMAHT (10 mg/ml in methanol) or MEH-PPV (5 mg/ml in toluene) onto glass slides at a rate of 2000 rpm producing films of ~10 and 50 μm, respectively. Photostability experiments were performed using the same experimental configuration used for PL measurements. Samples were irradiated using a Xe arc lamp (450 W) for 2 h at a specific excitation wavelength (450 nm for P3TMAHT and 500 nm for MEH-PPV). The integrated

emission intensity of the sample was measured at selected irradiation intervals. The irradiation power of the source was quantified using a photodiode (Newport, 818-VU-L detector) with an attached OD3 attenuator with a diameter of 50 μm, coupled to a Keithley 2401 Sourcemeter in two probe mode with Tracer2 software, yielding irradiance values of 231.4 W/m^2 at 450 nm and 166.1 W/m^2 at 500 nm, respectively.

Confocal microscopy was performed using a Carl Zeiss LSM700 confocal laser scanning system on an Axio Observer.Z1 inverted microscope stand with excitation wavelengths of 405 nm and 488 nm.

Fluorescence decays were measured using the picosecond time-correlated single photon counting (TCSPC) method at the Collaborative Optical Spectroscopy, Micromanipulation and Imaging Centre (COSMIC), University of Edinburgh, U.K. The excitation source was the second harmonic of the pulse-picked output of a Ti-Sapphire femtosecond laser system (Coherent, 10 W Verdi and Mira Ti-Sapphire), consisting of pulses of ~200 fs at 4.75 MHz repetition rate. Fluorescence decays were measured by an Edinburgh Instruments spectrometer equipped with TCC900 photon counting electronics. The instrument response of the system was ~50 ps FWHM. Fluorescence decay curves were analyzed using a standard iterative reconvolution method, assuming a multi-exponential decay function. CP-di-ureasils were excited at 365 nm and decays were recorded at emission wavelengths of 420 and 600 nm where the di-ureasil and CPs emit, respectively. CP stock solutions were excited at 460 nm, and the resulting fluorescence decays were recorded at 600 nm. Deconvolution of the fluorescence decays at 600 nm was performed using the Globals WE® software package.[56] However, for decays collected at 420 nm, the data could not be satisfactorily fitted at short times after the excitation pulse due to a significant contribution from light scattering. Thus, tail fits were also performed using DAS6 software (HORIBA). In each case the quality of fit was judged on the basis of the reduced chi-square statistic, χ^2, and the randomness of the residuals.

Supporting Information
Supporting Information is available from the Wiley Online Library or from the author.

Acknowledgements
The authors thank Antoine Lermoyer, Chloe Champion and John Carpenter for assistance with sample preparation and initial data collection. This work was supported in part by Science Foundation Ireland under Grant No. 12/IP/1608. NWF thanks the Irish Research Council for a Government of Ireland postgraduate studentship. The authors acknowledge financial support from the European Commission under the Seventh Framework Program by means of the grant agreement for the Integrated Infrastructure Initiative N. 262348 European Soft Matter Infrastructure (ESMI). Solid-state NMR spectra were obtained at the EPSRC UK National Solid-state NMR Service at Durham.

Received: ((will be filled in by the editorial staff))
Revised: ((will be filled in by the editorial staff))
Published online: ((will be filled in by the editorial staff))

[1] a) C. H. Duan, K. Zhang, X. Guan, C. M. Zhong, H. M. Xie, F. Huang, J. W. Chen, J. B. Peng, Y. Cao, *Chem. Sci.* **2013**, *4*, 1298; b) H. N. Kim, Z. Guo, W. Zhu, J. Yoon, H. Tian, *Chem. Soc. Rev.* **2011**, *40*, 79; c) A. Patra, M. Bendikov, S. Chand, *Acc.Chem. Res.* **2014**, *47*, 1465; d) P. Zalar, Z. B. Henson, G. C. Welch, G. C. Bazan, T. Q. Nguyen, *Angew. Chem. Int. Ed.* **2012**, *51*, 7495.

[2] M. C. Gather, A. Kohnen, K. Meerholz, *Adv. Mater.* **2011**, *23*, 233.

[3] L. Ying, C. L. Ho, H. Wu, Y. Cao, W. Y. Wong, *Adv. Mater.* **2014**, *26*, 2459.

[4] S. H. Wu, M. Aonuma, Q. S. Zhang, S. P. Huang, T. Nakagawa, K. Kuwabara, C. Adachi, *J. Mater. Chem. C* **2014**, *2*, 421.

[5] Y. S. L. V. Narayana, S. Basak, M. Baumgarten, K. Mullen, R. Chandrasekar, *Adv. Funct. Mater.* **2013**, *23*, 5875.

[6] H. Wu, L. Ying, W. Yang, Y. Cao, *Chem. Soc. Rev.* **2009**, *38*, 3391.

[7] B. H. Hamadani, S. Jung, P. M. Haney, L. J. Richter, N. B. Zhitenev, *Nano Lett*. **2010**, *10*, 1611.

[8] C. Duan, K. Zhang, C. Zhong, F. Huang, Y. Cao, *Chem. Soc. Rev*. **2013**, *42*, 9071.

[9] R. Trattnig, L. Pevzner, M. Jager, R. Schlesinger, M. V. Nardi, G. Ligorio, C. Christodoulou, N. Koch, M. Baumgarten, K. Mullen, E. J. W. List, *Adv. Funct. Mater*. **2013**, *23*, 4897.

[10] E. Ravindran, S. J. Ananthakrishnan, E. Varathan, V. Subramanian, N. Somanathan, *J. Mater. Chem. C* **2015**, *3*, 4359.

[11] S. Basak, M. A. Mohiddon, M. Baumgarten, K. Mullen, R. Chandrasekar, *Sci. Rep.* **2015**, *5*, 8406.

[12] Y. S. L. V. Narayana, M. Baumgarten, K. Müllen, R. Chandrasekar, *Macromolecules* **2015**, *48*, 4801−4812.

[13] M. Álvaro, A. Corma, B. Ferrer, M. S. Galletero, H. García, E. Peris, *Chem. Mater.* **2004**, *16*, 2142.

[14] a) R. C. Evans, *J. Mater. Chem. C* **2013**, *1*, 4190; b) R. C. Evans, A. G. Macedo, S. Pradhan, U. Scherf, L. D. Carlos, H. D. Burrows, *Adv. Mater.* **2010**, *22*, 3032; c) R. C. Evans, P. C. Marr, *Chem. Commun*. **2012**, *48*, 3742; d) T. Q. Nguyen, J. Wu, V. V. Doan, B. J. Schwartz, S. H. Tolbert, *Science* **2000**, *288*, 652.

[15] N. Willis-Fox, A. T. Marques, J. Arlt, U. Scherf, L. D. Carlos, H. D. Burrows, *Chem. Sci.* **2015**, DOI: 10.1039/c5sc02409a.

[16] L. D. Carlos, R. A. S. Ferreira, V. de Zea Bermudez, S. J. L. Ribeiro, *Adv. Funct. Mater.* **2001**, *11*, 111.

[17] V. de Zea Bermudez, L. D. Carlos, L. Alcacer, *Chem. Mater.* **1999**, *11*, 569.

[18] M. C. Goncalves, V. de Zea Bermudez, R. A. S. Ferreira, L. D. Carlos, D. Ostrovskii, J. Rocha, *Chem. Mater.* **2004**, *16*, 2530.

[19] M. E. Mesquita, S. S. Nobre, M. Fernandes, R. A. S. Ferreira, S. C. G. Santos, M. O. Rodrigues, L. D. Carlos, V. de Zea Bermudez, *J. Photochem. Photobio. A* **2009**, *205*, 156.

[20] A. Kaniyoor, B. McKenna, S. Comby, R. C. Evans, **2015**, submitted.

[21] P. P. Lima, R. A. S. Ferreira, S. A. Júnior, O. L. Malta, L. D. Carlos, *J. Photochem. Photobio. A* **2009**, *201*, 214.

[22] a) A. Gutacker, S. Adamczyk, A. Helfer, L. E. Garner, R. C. Evans, S. M. Fonseca, M. Knaapila, G. C. Bazan, H. D. Burrows, U. Scherf, *J. Mater. Chem*. **2010**, *20*, 1423; b) U. Scherf, A. Gutacker, N. Koenen, *Acc.Chem. Res.* **2008**, *41*, 1086.

[23] M. Knaapila, R. C. Evans, V. M. Garamus, L. Almasy, N. K. Szekely, A. Gutacker, U. Scherf, H. D. Burrows, *Langmuir* **2010**, *26*, 15634.

[24] L. D. Carlos, V. de Zea Bermudez, R. A. S. Ferreira, L. Marques, M. Assuncao, *Chem. Mater.* **1999**, *11*, 581.

[25] H. Y. Byun, I. J. Chung, H. K. Shim, C. Y. Kim, *Macromolecules* **2004**, *37*, 6945.

[26] L. Fu, R. A. S. Ferreira, M. Fernandes, S. C. Nunes, V. de Zea Bermudez, G. Hungerford, J. Rocha, L. D. Carlos, *Opt. Mater.* **2008**, *30*, 1058.

[27] L. Fu, R. A. S. Ferreira, N. J. O. Silva, L. D. Carlos, V. de Zea Bermudez, J. Rocha, *Chem. Mater*. **2004**, *16*, 1507.

[28] Scherrer equation: $L = 0.94\lambda/(A\cos\theta)$, where A (in radians) is the full-width-half-maximum of the Bragg peak. See A. Guinier, X-ray Diffraction in Crystals, Imperfect Crystals and Amorphous Bodies, Dover, New York 1994.

[29] P. P. Lima, S. A. Junior, O. L. Malta, L. D. Carlos, R. A. S. Ferreira, R. Pavithran, M. L. P. Reddy, *Eur. J. Inorg. Chem.* **2006**, *2006*, 3923.

[30] P. C. Barbosa, L. C. Rodrigues, M. M. Silva, M. J. Smith, *J. Power Sources* **2008**, *180*, 607.

[31] M. Fernandes, V. de Zea Bermudez, R. A. S. Ferreira, L. D. Carlos, N. V. Martins, *J. Lumin*. **2008**, *128*, 205.

[32] S. Chuangchote, T. Srikhirin, P. Supaphol, *Macromol. Rapid. Commun.* **2007**, *28*, 651.

[33] B. K. Kuila, A. K. Nandi, *J. Phys. Chem. B* **2006**, *110*, 1621.

[34] M. Jørgensen, K. Norrman, F. C. Krebs, Sol. Energ. Mat. Sol. Cells **2008,** *92*, 686.

[35] a) E. T. Hoke, I. T. Sachs-Quintana, M. T. Lloyd, I. Kauvar, W. R. Mateker, A. M. Nardes, C. H. Peters, N. Kopidakis, M. D. McGehee, *Adv. Energy Mater.* **2012**, *2*, 1351. b) C. Ran, M. Wang, W. Gao, J. Ding, Y. Shi, X. Song, H. Chen, Z. Ren, *J. Phys. Chem. C*, **2012**, *116*, 23053. c) X. Wang, L. C. Groff, J. D. McNeill, *Langmuir* **2013**, *29*, 13925.

[36] L. D. Carlos, R. A. S. Ferreira, R. N. Pereira, M. Assuncao, V. de Zea Bermudez*, J. Phys. Chem. B* **2004**, *108*, 14924.

[37] M. C. Neves, M. A. Martins, P. C. Soares-Santos, P. Rauwel, R. A. Ferreira, T. Monteiro, L. D. Carlos, T. Trindade, *Nanotechnology* **2008**, *19*, 155601.

[38] F. Kong, Y. M. Sun, R. K. Yuan, *Nanotechnology* **2007**, *18*, 265707.

[39] a) R. A. S. Ferreira, D. C. Oliveira, L. Q. Maia, C. M. S. Vicente, P. S. André, V. de Zea Bermudez, S. J. L. Ribeiro, L. D. Carlos, *Opt. Mater.* **2010**, *32*, 1587; b) D. C. Oliveira, A. G. Macedo, N. J. O. Silva, C. Molina, R. A. S. Ferreira, P. S. André, K. Dahmouche, V. de Zea Bermudez, Y. Messaddeq, S. J. L. Ribeiro, L. D. Carlos, *Chem. Mater.* **2008**, *20*, 3696.

[40] M. Wu, X. Xu, J. Wang, L. Li, *ACS Appl. Mater. Interfaces* **2015**, *7*, 8243.

[41] K. F. Karlsson, P. Asberg, K. P. R. Nilsson, O. Inganas, *Chem. Mater.* **2005**, *17*, 4204.

[42] L. Fu, R. A. S. Ferreira, N. J. O. Silva, A. J. Fernandes, P. Ribeiro-Claro, I. S. Gonçalves, V. de Zea Bermudez, L. D. Carlos, *J. Mater. Chem*. **2005**, *15*, 3117.

[43] H. D. Burrows, M. J. Tapia, C. L. Silva, A. A. Pais, S. M. Fonseca, J. Pina, J. S. de Melo, Y. Wang, E. F. Marques, M. Knaapila, A. P. Monkman, V. M. Garamus, S. Pradhan, U. Scherf, *J. Phys. Chem. B* **2007**, *111*, 4401.

[44] H. D. Burrows, V. M. M. Lobo, J. Pina, M. L. Ramos, J. S. de Melo, A. J. M. Valente, M. J. Tapia, S. Pradhan, U. Scherf, *Macromolecules* **2004**, *37*, 7425.

[45] R. C. Evans, M. Knaapila, N. Willis-Fox, M. Kraft, A. Terry, H. D. Burrows, U. Scherf, *Langmuir* **2012**, *28*, 12348.

[46] M. Knaapila, T. Costa, V. M. Garamus, M. Kraft, M. Drechsler, U. Scherf, H. D. Burrows, *J. Phys. Chem. B* **2015**, *119*, 3231.

[47] U. Balderas, C. Falcony, I. Moggio, E. Arias, M. Mondragón, *Polymer* **2013**, *54*, 2062.

[48] R. C. Evans, P. Douglas, *Anal. Chem*. **2006**, *78*, 5645.

[49] R. W. G. Hunt, *Measuring Colour*, Ellis Horwood, Chichester 1991.

[50] B. Ferreira, P. F. da Silva, J. S. S. de Melo, J. Pina, A. Macanita, *J. Phys. Chem. B* **2012**, *116*, 2347.

[51] A. T. Marques, H. D. Burrows, J. S. S. de Melo, A. J. Valente, L. L. Justino, U. Scherf, E. Fron, S. Rocha, J. Hofkens, E. W. Snedden, A. P. Monkman, *J. Phys. Chem. B* **2012**, *116*, 7548.

[52] T. Costa, A. T. Marques, J. S. S. de Melo, A. W. Thomas, L. E. Garner, U. Scherf, G. C. Bazan, H. D. Burrows, *J. Phys. Chem. B* **2014**, *118*, 613.

[53] T. Unger, F. Panzer, C. Consani, F. Koch, T. Brixner, H. Bassler, A. Kohler, *ACS Macro. Lett.* **2015**, *4*, 412.

[54] L. Zhai, R. D. McCullough, *Adv. Mater*. **2002**, *14*, 901.

[55] R. C. Evans, P. Douglas, *ACS Appl. Mater. Interfaces* **2009**, *1*, 1023.

[56] E. Gratton, J. Beechem, Globals WE (software), Laboratory for Fluorescence Dynamics, University of California, Irvine, CA 2004.

An efficient method for the fabrication of conjugated polymer (CP)-di-ureasil composite materials displaying tunable emission is presented. Judicious selection of the CP dopant concentration and the excitation wavelength facilitates modulation of the emission colour across the blue to yellow gamut, yielding white light with Commission Internationale de l'Eclairage (CIE) *xy* coordinates close to ideal white-light.

Keyword Conjugated Polymers, Hybrid Materials, Optically Active Materials; Photoluminescence, Composites

N. Willis-Fox, M. Kraft, J. Arlt, U. Scherf, R. C. Evans*

Tunable White-Light Emission from Conjugated Polymer-Di-ureasil Materials